

Controlled Grafting of Well-Defined Polymers on Hydrogen-Terminated Silicon Substrates by Surface-Initiated Atom Transfer Radical Polymerization

W. H. Yu, E. T. Kang,* and K. G. Neoh

Department of Chemical Engineering, National University of Singapore, Kent Ridge, Singapore 119260

Shiping Zhu

Department of Chemical Engineering, McMaster University, 1280 Main Street West, Hamilton, Ontario, Canada L8S 4L7

Received: February 8, 2003; In Final Form: July 1, 2003

Controlled grafting of well-defined polymer brushes on the hydrogen-terminated Si(100) substrates (the Si–H substrate) was carried out via the surface-initiated atom transfer radical polymerization (ATRP). Surface initiators were immobilized on the Si–H substrates in three consecutive steps: (i) coupling of an ω -unsaturated alkyl ester to the Si–H surface under UV irradiation, (ii) reduction of the ester groups by LiAlH₄, and (iii) esterification of the surface-tethered hydroxyl groups with 2-bromoisobutyrate bromide. Homopolymer brushes of methyl methacrylate (MMA), (2-dimethylamino)ethyl methacrylate (DMAEMA), and poly(ethylene glycol) monomethacrylate (PEGMA) were prepared by ATRP from the α -bromoester functionalized silicon surface. The chemical composition and topography of the graft-functionalized silicon surfaces were characterized by X-ray photoelectron spectroscopy (XPS) and atomic force microscopy (AFM), respectively. Kinetic studies revealed a linear increase in polymer film thickness with reaction time, indicating that chain growth from the surface was a controlled process with a “living” characteristic. Diblock copolymer brushes consisting of PMMA and PDMAEMA blocks were obtained by using the homopolymer brushes as the macroinitiators for the ATRP of the second monomer, providing further evidence to the existence of “living” chain ends. ATRP from the Si–H surfaces allowed the preparation of polymeric-inorganic hybrid materials with well-structured surface and interface.

1. Introduction

The manipulation and control of the physicochemical properties of single-crystal silicon surfaces are of crucial importance to the modern microelectronics industry.¹ A stable, densely packed organic layer covalently bonded to the silicon surface can be used, for example, as passivation layers in microfluidics and microelectromechanical systems (MEMS),² as recognition layers in sensors,³ and as an adhesion promoter for metals with the semiconductor substrate.⁴ One approach to this surface modification has been through the use of silane-based self-assembled monolayers (SAMs) on the native silicon oxide layer.⁵ Recently, a number of reports on the covalent attachment of organic monolayers to the oriented single-crystal silicon surface in the absence of the native oxide layer have appeared.^{6–11} The monolayers provide an opportunity for controlling the surface composition and architecture. However, the density of functional groups provided by the monolayers on a substrate surface is somewhat limited. To overcome this problem, surface initiated polymerization or graft polymerization has been carried out to covalently tether polymer brushes on the surfaces to increase the spatial density of the functional groups.^{12,13}

On the other hand, progress in polymerization techniques has made it possible to produce well-defined graft polymer chains on various surfaces. Polymerization methods that have been used to synthesize polymer brushes include cationic polymerization,¹⁴

anionic polymerization,^{15,16} ring-opening polymerization,^{17–19} radical polymerization,^{20–22} nitroxide-mediated radical polymerization,²³ atom transfer radical polymerization (ATRP),^{24–30} and reversible addition-fragmentation chain transfer polymerization (RAFT).³¹ ATRP is a recently developed “living” radical polymerization method, which is particularly versatile for the polymerization and block-copolymerization of various vinyl monomers, such as styrene, methacrylates, acrylates, and acrylonitrile.^{32,33} In addition, ATRP does not require stringent experimental conditions, as in the cases of anionic and cationic polymerization.

In the present work, immobilization of initiators on the hydrogen-terminated (100)-oriented single-crystal silicon (Si–H) surfaces for the preparation of well-defined polymer brushes is carried out. Initially, a highly stable monolayer tethered via Si–C bond to the silicon surface is obtained from the UV-induced coupling of 10-undecylenic methyl ester with the H–Si surface. Reduction of the ester group by LiAlH₄ yields a surface-tethered hydroxyl group, which can undergo esterifications with 2-bromoisobutyrate bromide. The tethered 2-bromoisobutyrate is used as the surface immobilized initiator for ATRP. Homopolymer brushes of methyl methacrylate (MMA), (2-dimethylamino)ethyl methacrylate (DMAEMA), and poly(ethylene glycol) monomethacrylate (PEGMA) are prepared by ATRP on the bromoester functionalized silicon surface. Diblock copolymer brushes consisting of PMMA and PDMAEMA blocks were prepared by using the homopolymer brushes as the macroinitiators for the ATRP of the second

* To whom all correspondence should be addressed. Tel.: +65-6874-2189. Fax: +65-6779-1936. E-mail address: cheket@nus.edu.sg.

monomer. The chemical composition and topography of the pristine and functionalized Si-H surfaces are determined by X-ray photoelectron spectroscopy (XPS) and atomic force microscopy (AFM), respectively.

2. Experimental Section

2.1. Materials. (100)-oriented single-crystal silicon, or Si(100), wafers, having a thickness of about 0.7 mm and a diameter of 150 mm, were obtained from Unisil Co. of Santa Clara, CA. The as-received wafers were polished on one side and doped as n-type. The silicon wafers were sliced into rectangular strips of about 1 cm \times 3 cm in size. To remove the organic residues on the surface, the silicon substrate was washed with the "piranha" solution, a mixture of 98 wt % concentrated sulfuric acid (70 vol %) and hydrogen peroxide (30 vol %).³⁴ **Caution: Piranha solution reacts violently with organic materials and should be handled carefully!** After being rinsed with copious amounts of doubly distilled water, the Si(100) strips were blown dry with purified argon. The clean Si(100) strips were immersed in 10 vol % hydrofluoric acid solution in individual Teflon vials for 5 min to remove the oxide film and to leave behind a hydrogen-terminated Si(100) surface (Si-H surface).

All the chemical reagents were purchased from Aldrich Chemical Co. of Milwaukee, WI. Methyl methacrylate (MMA) and (2-dimethylamino)ethyl methacrylate (DMAEMA) were distilled under reduced pressure and stored in an argon atmosphere at $-10\text{ }^{\circ}\text{C}$. Poly(ethylene glycol) monomethacrylate (PEGMA) macromonomer ($M_n \sim 360$) was passed through the silica gel column to remove the inhibitor. It was also stored under an argon atmosphere at $-10\text{ }^{\circ}\text{C}$. 10-Undecylenic acid methyl ester was prepared according to the method described in the literature.⁷ Diethyl ether was distilled over LiAlH_4 before use. Copper(I) bromide and copper(I) chloride were purified according to procedures described in the literature.²⁶ Ethyl bromoisobutyrate (EBiB), 1,1,4,7,10,10-hexamethyltriethylenetetramine (HMTETA), 2,2'-bipyridine (Bpy), and other chemical reagents were used without further purification.

2.2. Immobilization of the Initiator on the Hydrogen-Terminated Silicon Surface. Immobilization of the initiator on the Si-H surface was achieved through (i) UV-induced coupling of 10-undecylenic methyl ester with the Si-H surface, (ii) reduction of the ester group of the monolayer on the silicon surface by LiAlH_4 , and (iii) esterification of the tethered hydroxyl groups with 2-bromoisobutyrate bromide. The three-step immobilization process is shown schematically in Figure 1.

For the UV-induced coupling reaction on the Si-H surface, a small amount of liquid 10-undecylenic acid methyl ester was introduced onto the freshly prepared Si-H surface. The substrate was sandwiched between two quartz plates. Thus, the Si-H surface was wetted by a uniform liquid film of the ω -unsaturated alkyl ester. The assembly was placed in a Pyrex tube and subjected to UV irradiation in a Riko rotary photochemical reactor (model RH400-10W, manufactured by Riko Denki Kogyo of Chiba, Tokyo) at $25\text{ }^{\circ}\text{C}$ for 2 h. The reactor was equipped with a 1000 W Hg lamp. The surface-modified silicon substrate was separated from the quartz plates and washed thoroughly with copious amounts of acetone to remove the residual ω -unsaturated alkyl ester. Finally, the alkyl ester-modified silicon substrate (the Si-R₁COOCH₃ substrate) was dried by pumping under reduced pressure for about 10 h.

For the reduction of the ester terminated monolayer on the silicon surface, 100 mL of ether was added to a dry flask,

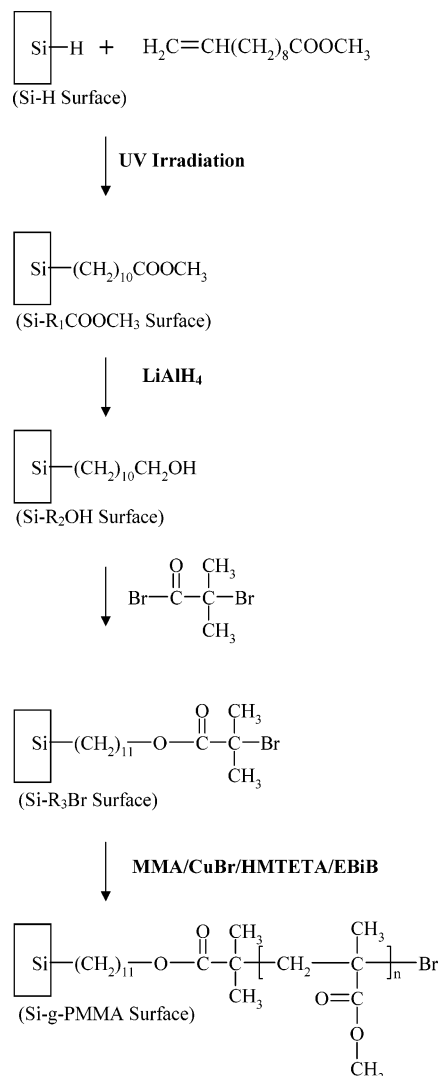


Figure 1. Schematic diagram illustrating the processes of UV-induced coupling of 10-undecylenic acid methyl ester on the Si-H surface, reduction of the ester-functionalized silicon surface, formation of the 2-bromoisobutyrate-functionalized silicon surface, and surface graft polymerization via ATRP from the bromoester-functionalized silicon surface.

followed by degassing with purified argon. About 5 g of LiAlH_4 powder was added slowly into the flask with stirring. Three pieces of the Si-R₁COOCH₃ substrates were then immersed in the solution. The reaction mixture was left to stand for 2 h at room temperature. The so-modified silicon substrates (the Si-R₂OH substrates) were removed from the reaction mixture and washed thoroughly with acetone, 0.5 M HCl solution, acetone, and water, in that order. The Si-R₂OH substrates were dried by pumping under reduced pressure for about 10 h.

For the esterification reaction, to a solution of 1.5 mL of pyridine in 50 mL of dry ether was added 3 pieces of the Si-R₂OH substrates, followed by dropwise addition of 2 mL of 2-bromoisobutyryl bromide in 30 mL of dry ether over 30 min. The reaction mixture was gently stirred at $0\text{ }^{\circ}\text{C}$ for 2 h, and then at room temperature for another 10 h. The so-modified silicon substrates (the Si-R₃Br substrates) were removed and washed with ethanol, and water. The substrates were then dried by pumping under reduced pressure for about 10 h.

2.3. Surface Initiated Atom Transfer Radical Polymerization. For the preparation of poly(methyl methacrylate) (PMMA) brushes on the Si-R₃Br surface, MMA (4 mL, 37.4 mmol), CuBr (18 mg, 0.125 mmol), and HMTETA (34 μL ,

0.125 mmol) were added to 4 mL of a mixed solvent (anisole:acetonitrile, 1:1, v/v). The solution was stirred and degassed with argon for 20 min. The Si-R₃Br substrate and the free initiator, EBiB (18 μ L, 0.125 mmol), were then added to the solution. The reaction flask was sealed and kept in a 70 °C oil bath for a predetermined period of time. After the reaction, the silicon substrate with surface grafted poly(methyl methacrylate) (the Si-g-PMMA surface) was removed from the solution and washed thoroughly with excess acetone. The “free” PMMA formed in the solution by the free initiator was recovered by precipitating in excess methanol. Monomer conversion was determined gravimetrically.

For the preparation of poly((2-dimethylamino)ethyl methacrylate) (PDMAEMA) brushes on the Si-R₃Br surfaces, DMAEMA (5 mL, 30 mmol), CuBr (22 mg, 0.15 mmol), and HMTETA (41 μ L, 0.15 mmol) were added to 5 mL of THF. The mixture was stirred and purged with argon for 20 min. The Si-R₃Br substrate and EBiB (22 μ L, 0.15 mmol) were then introduced into the solution. The reaction flask was sealed and placed in a 60 °C water bath for a predetermined period of time. After the reaction, the silicon substrate with surface grafted PDMAEMA (the Si-g-PDMAEMA surface) was removed from the reaction mixture and washed thoroughly with excess ethanol. The free PDMAEMA was recovered by precipitating in excess petroleum ether.

For the preparation of poly(poly(ethylene glycol) monomethacrylate) (PPEGMA) brushes on the Si-R₃Br surfaces, PEGMA (15 mL, 45 mmol), CuCl (45 mg, 0.45 mmol), CuCl₂ (12 mg, 0.09 mmol), and Bpy (168 mg, 1.08 mmol) were added to 10 mL of doubly distilled H₂O. The mixture was stirred and purged with argon for 20 min. The Si-R₃Br substrate was then introduced into the solution. The reaction flask was sealed and placed in a 25 °C water bath for a predetermined period of time. After the reaction, the silicon substrate with surface grafted PPEGMA (the Si-g-PPEGMA surface) was removed from the reaction mixture and washed thoroughly with excess doubly distilled water.

For the preparation of the PDMAEMA-*b*-PMMA copolymer brushes on the Si-R₃Br surfaces, the Si-g-PMMA substrate (or the Si-g-PDMAEMA substrate) was used instead of the Si-R₃Br substrate for ATRP of DMAEMA (or MMA) under the same polymerization condition as described above.

2.4. Materials and Surface Characterization. The chemical composition of the pristine and the functionalized Si-H surfaces was determined by X-ray photoelectron spectroscopy (XPS). The XPS measurements were performed on a Kratos AXIS HSi spectrometer using a monochromatic Al K α X-ray source (1486.6 eV photons) at a constant dwell time of 100 ms and a pass energy of 40 eV. The samples were mounted on the standard sample studs by means of double-sided adhesive tapes. The core-level signals were obtained at a photoelectron takeoff angle (α , measured with respect to the sample surface) of 90°. The X-ray source was run at a reduced power of 150 W (15 kV and 10 mA). The pressure in the analysis chamber was maintained at 10⁻⁸ Torr or lower during each measurement. All binding energies (BE's) were referenced to the C 1s hydrocarbon peak at 284.6 eV. Surface elemental stoichiometries were determined from the spectral area ratios, after correcting with the experimentally determined sensitivity factors, and were reliable to within $\pm 10\%$. The elemental sensitivity factors were calibrated using stable binary compounds of well-established stoichiometries.

The topography of the pristine and graft-polymerized silicon surfaces was studied by atomic force microscopy (AFM), using

a Nanoscope IIIa AFM from the Digital Instrument Inc. In each case, an area of 5 \times 5 μ m square was scanned using the tapping mode. The drive frequency was 330 \pm 50 kHz, and the voltage was between 3 and 4.0 V. The drive amplitude was about 300 mV, and the scan rate was 0.5–1.0 Hz. An arithmetic mean of the surface roughness (R_a) was calculated from the roughness profile determined by AFM.

Gel permeation chromatography (GPC) measurements were carried out using an HP 1100 HPLC equipped with a PLgel 5 μ m MIXED-C column and a HP 1047A refractive index detector. THF was used as the mobile phase for PMMA, and THF with 2 vol % triethylamine was used for PDMAEMA.³⁵ Monodispersed polystyrene standards (Polymer Lab, Agilent Co.) were used to generate the calibration curve.

The thickness of the polymer films grafted on the silicon substrates was determined by ellipsometry. The measurements were carried out on a variable angle spectroscopic ellipsometer (model VASE, J. A. Woollam Inc., Lincoln, NE) at an incident angles of 70° and 75° in the wavelength range 250–1000 nm. The refractive index of the dried films at all wavelengths was assumed to be 1.5. All measurements were conducted in the dry air at room temperature. For each sample, thickness measurements were made on at least three different surface locations. Each thickness reported was reliable to ± 1 nm. Data were recorded and processed using the WVASE32 software package.

Static water contact angles of the pristine and functionalized Si-H surface were measured at 25 °C and 60% relative humidity by the sessile drop method, using a 3 μ L water droplet in a telescopic goniometer (Rame-Hart, Model 100-00-(230), manufactured by the Rame-Hart, Inc., Mountain Lakes, NJ). The telescope with a magnification power of 23 \times was equipped with a protractor of 1° graduation. For each sample, at least three measurements from different surface locations were averaged. Each angle reported was reliable to $\pm 3^\circ$.

3. Results and Discussion

3.1. Immobilization of Initiator on the Hydrogen-Terminated Silicon Surface. To prepare the polymer brush on the silicon surface, a uniform and dense layer of initiators immobilized on the silicon surface is indispensable. The chemical composition of the pristine Si(100) surface and the silicon surface at various stages of surface modification was determined by XPS. Two peak components at the binding energies (BE's) of about 99 and 103 eV, attributable to the Si-Si and Si-O species, respectively, are observed in the Si 2p core-level spectrum of the pristine Si(100) surface, as shown in Figure 2a. Treatment of the pristine Si(100) surface with dilute HF removes the native oxide layer and yields the Si-H surface.¹ The disappearance of the Si-O species at the BE of 103 eV confirms that the silicon surface is ideally hydrogen-terminated after the HF treatment (Figure 2b).

Coupling of the ester group-terminated monolayers to the Si-H surfaces was performed using the well-established technique.^{6–11} Previous studies have shown that an alkyl monolayer can be tethered covalently to the hydrogen-terminated Si(100) or Si(111) surface via the use of a radical initiator or a metal complex catalyst, as well as via thermal activation, photoirradiation, or electrochemical reaction.¹ A radical-chain mechanism is proposed in the previous studies.⁶ The surface Si-H group is homolytically dissociated (for instance, by UV irradiation) to form the radical site (a dangling bond), which reacts readily with an alkene to form a surface-tethered alkyl radical on the β -carbon. This radical, in turn, abstracts a hydrogen atom from

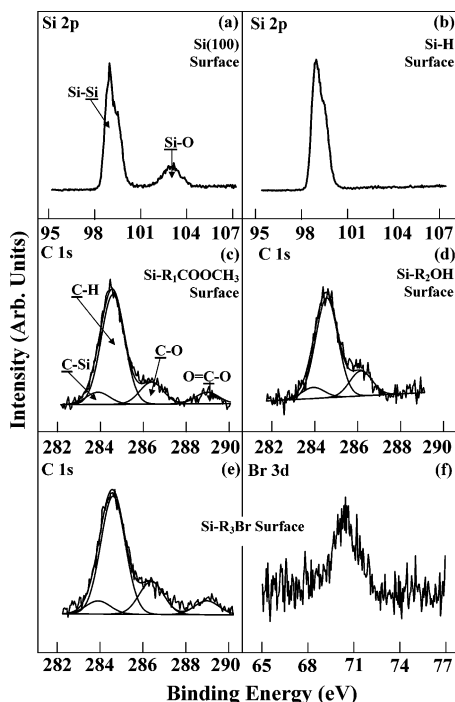


Figure 2. XPS Si 2p core-level spectra of (a) the pristine Si(100) and (b) the Si-H surface, C 1s core-level spectra of (c) the Si-R₁COOCH₃ surface and (d) the Si-R₂OH surface, and (e) C 1s and (f) Br 3d core-level spectra of the Si-R₃Br surface.

an adjacent Si-H bond. Abstraction of a neighboring hydrogen atom completes the hydrosilylation process and creates another reactive silicon radical. The reaction propagates subsequently as a chain reaction on the Si-H surface.⁸ Figure 2c shows the C 1s core-level spectrum of the Si-H surface after being subjected to UV irradiation for 2 h in the presence of 10-undecylenic acid methyl ester. The C 1s core-level spectrum of the ester functionalized silicon surface (the Si-R₁COOCH₃ surface) can be curve-fitted with four peak components having BE's at about 283.9, 284.6, 286.4, and 288.8 eV, attributable to the Si-C species, C-H species, the C-O species, and the O=C-O species, respectively.^{36,37} A [Si-C]:[C-H]:[C-O]:[O=C-O] ratio of 1:9:1.8:1 is obtained for the Si-R₁COOCH₃ surface. The deviation from the theory ratio of 1:9:1:1 is probably due to photooxidation of the formed monolayer by the UV source. Nevertheless, the closely preserved proportion of the O=C-O species allows the subsequent surface functionalization.

The Si-R₁COOCH₃ surface was then reduced by LiAlH₄ in dry ether to give rise to the hydroxyl-terminated silicon surface (Si-R₂OH surface). A very hydrophilic surface (with a water contact angle of only about 30°) was obtained after the subsequent cleaning of the modified surface with acetone, dilute HCl solution, acetone and water, in that order. The disappearance of the O=C-C peak component (see Figure 2d) in the C 1s core-level spectrum of the Si-R₂OH surface indicates the ester group is reduced to the hydroxyl group.⁷

The presence of the Br 3d core-level spectrum at the BE of around 70.5 eV and the reappearance of the O=C-O peak component in the C 1s core-level spectrum of the 2-bromoisobutyrate functionalized silicon surface (the Si-R₃Br surface) indicate that the 2-bromoisobutyrate species has been successfully immobilized on the silicon surface. The respective C1s and Br 3d core-level spectra of the Si-R₃Br surface are shown in Figures 2e,f.

The thickness of the coupled monolayer on the Si-R₁-COOCH₃ surface, as determined by optical ellipsometry, is about 1.7 nm, which is comparable to that of the ester-terminated monolayer on the Si-H surface from thermal coupling.⁷ The persistence of very strong Si signals in the wide scan spectrum of the Si-R₁COOCH₃ surface provides additional evidence to the fact that the thickness of the monolayer is much less than the sampling depth of the XPS technique (about 7.5 nm in an organic matrix³⁸). After immobilization of the 2-bromoisobutyrate segments, the thickness of the monolayer on the Si-R₃Br surface increases to about 2.5 nm.

3.2. Surface Initiated Polymerization from the α -Bromoester Functionalized Silicon Surface via ATRP. The advantage of ATRP over other living polymerization, such as anionic and cationic polymerization, is the tolerance for various functionalities in the monomers, leading to polymers with functionalities along the chains. Therefore, the physicochemical properties of the silicon surface can be tuned by the choice of a variety of vinyl monomers. In addition to the selection of MMA as the model monomer, two additional functional monomers, DMAEMA and PEGMA, are also selected. The DMAEMA polymer is both thermal-sensitive and pH-sensitive.³⁹ The well-defined PDMAEMA brush can be used to prepare a "smart" surface on a nanometer scale, because they react collectively to environmental stimuli, such as changes in pH or temperature. The PEGMA polymer-grafted silicon surface from conventional radical polymerization was effective in preventing protein adsorption and platelet adhesion.⁴⁰ A biocompatible silicon surface prepared from PEGMA graft polymerization can be used in the silicon-based biomedical microdevices. Furthermore, the hydroxyl end groups of the grafted poly(ethylene glycol) side chains can also be converted into various functional derivatives.⁴¹

A sufficient concentration of the deactivating Cu(II) complex is necessary to rapidly establish an equilibrium between the dormant and the active chains at the begin of ATRP. In the absence of this controlled equilibrium, the process resembles that of the conventional redox-initiated radical polymerization.^{32,33} The Cu(II) species can be obtained by the reaction of Cu(I) complex with the initiator to produce the active radical for propagation, or by addition at the begin of reaction. The main difference between ATRP from a surface and ATRP in bulk or solution is the relatively low concentration of the initiator immobilized on the surface. The low surface initiator concentration can lead to a low concentration of the deactivating species (Cu(II) complex) being formed at the begin of polymerization. The problem can be resolved by two approaches. One is the addition of the free initiator at the begin of the reaction,²⁴ and the other is the addition of the deactivator (Cu(II) complex).²⁶ Because of the difficulty in obtaining the molecular weight of the grafted polymer on the silicon surface, the first approach was chosen to control the ATRP from the surface. In addition, the "free" polymer formed by the free initiator in solution can be used to monitor the properties of the grafted polymer. Thus, the free initiator serves not only as a mediator for ATRP on the surface, but also as an indicator of surface graft polymerization.

Initial experiments using anisole as solvent for ATRP from the Si-R₃Br surface did not yield good results. Copper precipitation on the flask wall was observed at high conversion when the [monomer]/[initiator] ratio was increased to 300. The coverage of the PMMA brushes on the silicon surface was very low. Previous studies have shown that the use of polar solvents for ATRP can result in an increase in polymerization rate and dissolution of the copper complex.^{33,42} Thus, a mixed solvent

TABLE 1: Chemical Compositions, Contact Angle, Film Thickness, and Surface Coverage of the Graft-Polymerized Silicon Surfaces

sample	chemical composition			static contact angle ($\pm 3^\circ$)	film thickness (± 1 nm)	surface coverage ^c (mg/m ²)
	[O]/[C] ^a	[N]/[C] ^a	[C-H]:[C-O]:[O=C-O] or [C-H]:[C-N]:[C-O]:[O=C-O] ^b			
Si-g-PMMA surface ^d	0.38 (0.4)	0.0 (0.0)	2.8:1:1 (3:1:1)	70	9.5	10.5
Si-g-PDMAEMA surface ^e	0.22 (0.25)	0.12 (0.125)	3.2:3:1:1 (3:3:1:1)	48	15	15.0
Si-g-PPEGMA surface ^f	0.44 (0.5)	0.0 (0.0)	2.7:8:1 (3:12:1)	44	23	23.0

^a Determined from XPS core-level spectral area ratio. Values in parentheses are the theoretical ratios. ^b Determined from the XPS curve-fitted C 1s core-level spectra. Values in parentheses are the theoretical ratios. [C-H]:[C-O]:[O=C-O] ratio for the Si-g-PMMA and Si-g-PPEGMA surfaces. [C-H]:[C-N]:[C-O]:[O=C-O] ratio for the Si-g-PDMAEMA surface. ^c Surface coverage = film thickness \times density. (1.1 g/cm³ for PMMA, 1.0 g/cm³ for PDMAEMA and PPEGMA). ^d Reaction conditions: [MMA]:[EBiB]:[CuBr]:[HMTETA] = 300:1:1:1, [MMA] = 4.7 M, solvent anisole/acetonitrile = 1/1 (v/v), temp 70 °C, reaction time 5 h. ^e Reaction conditions: [DMAEMA]:[EBiB]:[CuBr]:[HMTETA] = 200:1:1:1, [DMAEMA] = 3 M, solvent THF, temp 60 °C, reaction time 5 h. ^f Reaction conditions: [PEGMA]:[CuCl]:[CuCl₂]:[Bpy] = 100:1:0.2:2.4, [PEGMA] = 1.8 M, solvent water, temp 25 °C, reaction time 2 h.

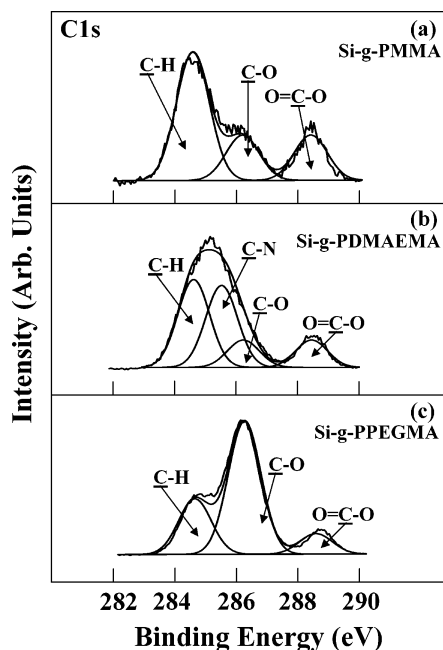


Figure 3. XPS C1s core-level spectra of the Si-R₃Br surface subjected to ATRP of (a) MMA, (b) DMAEMA, and (c) PEGMA. Reaction conditions are shown in Table 1.

(anisole: acetonitrile = 1:1, v/v) was chosen for carrying out the ATRP of MMA on the Si-R₃Br surface. No copper precipitation was observed during ATRP. The reaction medium remains homogeneous throughout the polymerization process.

The presence of grafted polymer on the silicon surface is ascertained first by XPS analysis. The results are shown in Figure 3. The C 1s core-level spectra of the Si-g-PMMA surface (part a) and Si-g-PPEGMA surface (part c) can be curve-fitted with three peak components having BE's at about 284.6, 286.2, and 288.5 eV, attributable to the C-H, C-O, and O=C-O species, respectively.^{36,37} On the other hand, the C 1s core-level spectrum of the Si-g-PDMAEMA surface can be curve-fitted with four peak components having BE's at about 284.6, 285.5, 286.2, and 288.5 eV, attributable to the C-H, the C-N, the C-O, and the O=C-O species, respectively.^{36,37}

Table 1 summarizes the surface analysis results of the MMA, DMAEMA, and PEGMA graft polymerized silicon substrates via ATRP. For the MMA homopolymer, the theoretical [O]/[C] ratio and [CH]:[C-O]:[O=C-C] ratio are 0.4 and 3:1:1, respectively. As shown in Table 1, the [O]/[C] ratio and the [CH]:[C-O]:[O=C-C] ratio of the Si-g-PMMA surface,

obtained from XPS analysis, are in fairly good agreement with the respective theoretical ratios. Fairly good agreement between the XPS-derived and theoretical surface composition is also observed for the PDMAEMA and PPEGMA grafted silicon surface. The surface coverage is defined as the amount of the grafted polymer per square meter of the surface and is calculated from the product of thickness and density of the grafted polymer layer. For simplicity, the density of the corresponding bulk polymer is used as the density of the grafted polymer film. Thus, surface coverages of 10.5, 15, and 23 mg/m² were obtained, respectively, for the PMMA, PDMAEMA, and PPEGMA brushes on the silicon surfaces, as shown in Table 1. For the Si-g-PMMA surface, the surface coverage is comparable to that previously reported for the PMMA brushes grown from the native (oxides-covered) silicon surface via ATRP.³⁰

The variation in water contact angle for the silicon surfaces with different polymer brushes indicates that the hydrophilicity of the silicon surface can be easily tuned. The contact angle of the pristine Si-H surface is about 72°. After immobilization of the 2-bromoisobutyrate terminated monolayer, the contact angle is about 65°. As shown in Table 1, the silicon surface with a PMMA graft layer (at a thickness of 9.5 nm) has a contact angle of about 70°. When grafted with a PPEGMA layer, the silicon surface becomes more hydrophilic and the contact angle decreases to about 44°.

The ellipsometry measurements indicate a large increase in film thickness after the growth of the PMMA layer on the Si-R₃Br surface. Control experiments, under the conditions similar to that for surface graft polymerization via ATRP, are carried on the following surfaces: the Si-H surface, the Si-R₁COOCH₃ surface, and the Si-R₂OH surface. No increase in thickness on all the control surfaces was discernible. The results confirm that the increase in thickness observed is the result of graft polymerization from the 2-bromoisobutyrate functionalized silicon surface, or the Si-R₃Br surface. Furthermore, because ATRP is a "living" polymerization process, the thickness of the polymer brushes should increase linearly with the polymerization time and the molecular weight of the graft polymer.

As shown in Figure 4a, an approximately linear increase in thickness of the grafted PMMA layer on the Si-R₃Br surface with the polymerization time is observed. The deviation might have been caused by the nanoscaled phase aggregation of the grafted polymer after the surface has been dried (see AFM data below). A linear relationship between the thickness of the PMMA layer and the molecular weight of the "free" polymer

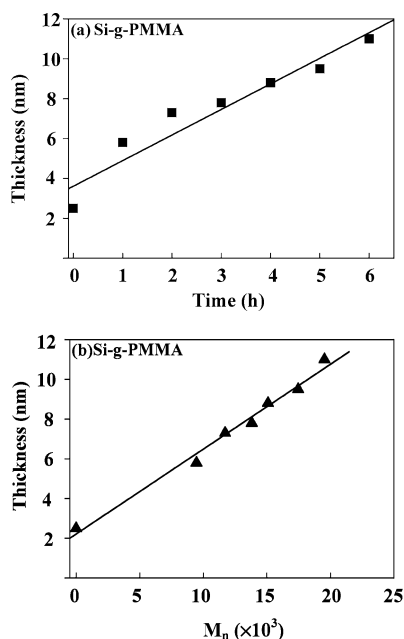


Figure 4. Dependence of the thickness of the PMMA layer, grown from the Si- R_3 Br surface via ATRP, on (a) polymerization time and (b) molecular weight (M_n) of the “free” PMMA formed in the solution. Reaction conditions: [MMA]:[EBiB]:[CuBr]:[HMTETA] = 300:1:1:1, [MMA] = 4.7 M, solvent anisole/acetonitrile = 1/1 (v/v), temp 70 °C.

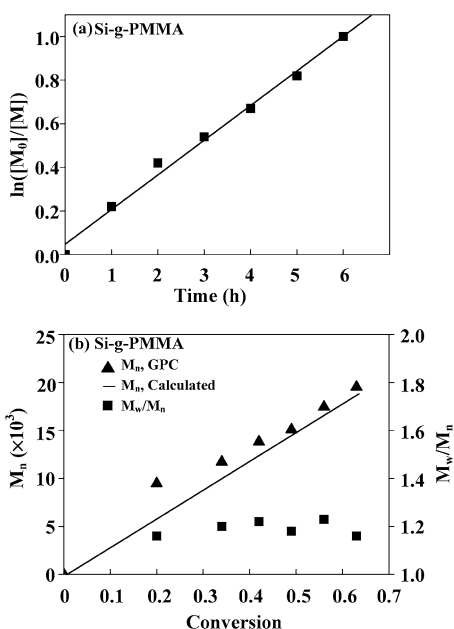


Figure 5. The relationships (a) between $\ln([M_0]/[M])$ and polymerization time and (b) between M_n and monomer conversion (see Figure 4 for reaction conditions)

formed in the solution is also observed (Figure 4b). Although the exact molecular weight of the polymer grafted on the silicon surface is not known, the molecular weight of the graft polymer is expected to be proportional to that of the polymer formed in the solution.^{24,26} These results indicate that the process of surface initiated ATRP of MMA is controlled.

Additional evidence on the controlled polymerization is also obtained from the “free” PMMA formed by the free initiator. Figure 5a shows the linearity relationship between $\ln([M_0]/[M])$ and time, where $[M_0]$ is the initial monomer concentration and $[M]$ is the monomer concentration. The result indicates that the concentration of the growing species remains constant and a

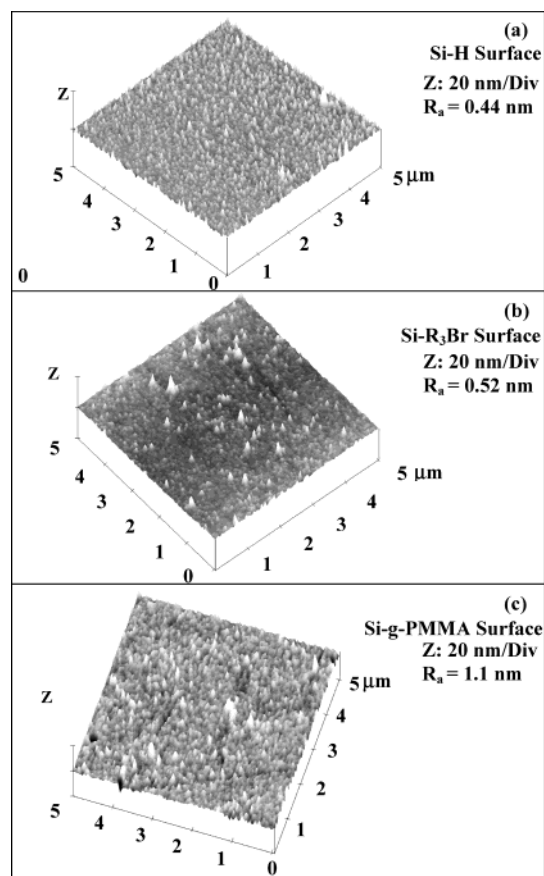


Figure 6. AFM images of (a) the Si-H surface, (b) the Si- R_3 Br surface, and (c) the Si-g-PMMA surface (PMMA thickness = 9.5 nm).

first-order kinetic is obtained. Figure 5b shows the relationship between M_n of the free PMMA and the conversion of the MMA monomer. The number-average molecular weight of the “free” PMMA increases linearly with the increase in monomer conversion. The polydispersity index (M_w/M_n) of the free PMMA is also around 1.2.

3.3. Surface Topography. The changes in topography of the silicon surfaces after modification by ATRP surface graft polymerization were studied by AFM. Representative AFM images of the pristine Si-H, Si- R_3 Br, and Si-g-PMMA (PMMA thickness of 9.5 nm) surfaces are shown in Figure 6. The root-mean-square surface roughness (R_a) of the pristine Si-H surface is only about 0.44 nm. The Si- R_3 Br surface remains molecularly uniform with an R_a value of about 0.52 nm. After surface graft polymerization of MMA via ATRP, the R_a value increases slightly to about 1.1 nm. In addition, the ellipsometry data indicate that the grafted PMMA film exhibits nanoscopic uniformity in thickness. These results suggest that the ATRP graft polymerization has proceeded uniformly on the Si- R_3 Br surface to give rise to a dense coverage of PMMA on the silicon surface. As is also shown in Figure 6c, the grafted MMA polymer chains on the silicon surface exist as a distinctive overlayer. The formation of the nanosized islands probably has resulted from the nanoscaled phase aggregation of the grafted polymer after the surface has been dried.

3.4. Block Copolymer Brushes. Another advantage of ATRP over the conventional radical polymerization technique is the possibility for the synthesis of block copolymers. ATRP is used to synthesize the PMMA-*b*-PDMAEMA diblock copolymer brushes from the α -bromoester functionalized silicon surface.

The formation of block copolymer brushes was confirmed by the ellipsometry and XPS. A 7 nm increase in the thickness

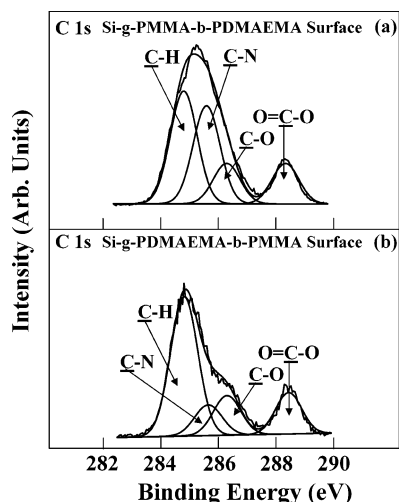


Figure 7. XPS C 1s core-level spectra of (a) the MMA-*b*-DMAEMA and (b) DMAEMA-*b*-MMA block copolymer brushes on the silicon surface (the thickness values of the initial homopolymer and block copolymer brushes are given in Table 2).

of the grafted polymer layer was observed by ellipsometry after ATRP of DMAEMA at 60 °C for 6 h on the Si-g-PMMA surface (initial thickness 9.5 nm). Figure 7a shows the XPS C 1s core-level spectrum of the Si-g-PMMA-*b*-PDMAEMA surface. In comparison with the C 1s core-level spectrum of the Si-g-PMMA surface shown in Figure 3a, a new peak component, assigned to the C–N species, appears in the curve-fitted C 1s core-level spectrum of the Si-g-PMMA-*b*-PDMAEMA surface. In addition, a new N 1s peak component at the BE of 398.5 eV has also appeared in the wide scan spectrum of the Si-g-PMMA-*b*-PDMAEMA surface. These results confirm that some of the dormant sites at the ends of the grafted PMMA chains allow the reactivation of the graft polymerization process, resulting in the formation of the block copolymer brushes on the silicon surface. The C–N peak component arises solely from the PDMAEMA block of the PMMA-*b*-PDMAEMA copolymer brush. The peak component areas of the C–H and C–N species are also expected to be equal for the PDMAEMA block. The fact that the C 1s core-level line shape in Figure 7a closely resembles that of the Si-g-PDMAEMA surface in Figure 3b ready confirms that the Si-g-PMMA-*b*-PDMAEMA surface is dominated by the PDMAEMA blocks and the PMMA blocks are located mostly below the sampling depth of the XPS technique (about 7.5 nm in an organic matrix³⁸). The ratio of the PMMA blocks to the PDMAEMA blocks within the XPS sampling depth can, nevertheless, be determined from the $[C-H]_{PMMA}/[C-H]_{PDMAEMA}$ ratio, or the $([C-H] - [C-N])/[C-N]$ ratio in Figure 7a. The result is given in Table 2.

The water contact angles of the diblock polymer brushes on the silicon surfaces are also shown in Table 2. After DMAEMA has been block-copolymerized onto the PMMA brushes, the contact angle of the Si-g-PMMA-*b*-PDMAEMA surface decreases from about 70 to 50°. The contact angle is comparable to that of the homopolymer brushes of PDMAEMA on the silicon surface.

In another example, a Si-g-PDMAEMA surface with 15 nm thick PDMAEMA was used for the ATRP of MMA. A 5 nm increase in thickness of the grafted polymer layer was measured by ellipsometry after ATRP of MMA at 70 °C for 4 h from the Si-g-PDMAEMA surface. In comparison with the C 1s core-level spectrum of the Si-g-PDMAEMA surface shown in Figure 3b, a substantial decrease in peak component area of the C–N

TABLE 2: Contact Angle, Film Thickness, and Surface Composition of the Diblock Copolymer Brushes Grafted on the Hydrogen-Terminated Silicon Surfaces via ATRP

sample	contact angle (± 3°)	thickness (± 1 nm)	surface composition ^a	
			PMMA (mol %)	PDMAEMA (mol %)
Si-g-PMMA- <i>b</i> -PDMAEMA surface ^b	50	16.5	14	86
Si-g-PDMAEMA- <i>b</i> -PMMA surface ^c	65	20	76	24

^a Determined from the curve-fitted XPS C 1s core-level spectra.

^b Surface ATRP of DMAEMA from the Si-g-PMMA surface (PMMA thickness = 9.5 nm). ^c Surface ATRP of MMA from the Si-g-PDMAEMA surface (PDMAEMA thickness = 15 nm).

species is observed in the C 1s core-level spectrum of the Si-g-PDMAEMA-*b*-PMMA surface (Figure 7b). The ratio of the PMMA blocks to the PDMAEMA blocks on the Si-g-PDMAEMA-*b*-PMMA surface was found to be about 3:1, as determined from the C–H and C–N peak component areas in Figure 7b. The result is given in Table 2. The smaller thickness (than the sampling depth of the XPS technique) of the PMMA blocks allows a higher proportion of the underlying PDMAEMA blocks to be detected by the XPS technique. Finally, as shown in Table 2, the water contact angle of the Si-g-PDMAEMA-*b*-PMMA surface is also comparable to that of the Si-g-PMMA surface.

4. Conclusions

Controlled grafting of well-defined polymer brushes of PMMA, PDMAEMA, and PPEGMA was carried out via ATRP on the hydrogen-terminated Si(100) surfaces (the Si–H surfaces). Prior to the surface initiated ATRP, the Si–H surface was functionalized by the α -bromoester group in three steps: coupling of an ω -unsaturated alkyl ester with the Si–H surface under UV irradiation, reduction of the ester group by LiAlH₄, and esterification of the surface-tethered hydroxyl group with 2-bromoisobutyrate bromide. XPS and ellipsometry data indicated the formation of polymer brushes on the silicon surface. Kinetic studies revealed a linear increase in thickness of the surface graft polymerized film with reaction time and M_n of the homopolymer in solution, indicating that the chain growth from the surface was a controlled process with a “living” characteristic. AFM images suggested that the surface graft polymerization via ATRP had proceeded uniformly on the α -bromoester functionalized silicon surface. Diblock copolymer brushes consisting of PMMA and PDMAEMA blocks were obtained on the silicon surfaces using either type of the homopolymer brushes as the macroinitiators for ATRP of the second monomer. The homopolymer and block copolymer covalently tethered to the silicon atoms at the surfaces have imparted new and well-structured functionalities directly onto the inorganic single-crystal surfaces.

References and Notes

- (1) Buriak J. M. *Chem. Rev.* **2002**, *102*, 1272.
- (2) Zhu, X. Y. *Acta Phys.-Chem. Sin.* **2002**, *18*, 855.
- (3) Ji, H. F.; Thundat, T.; Dabestani, R.; Brown, G. M.; Britt, P. F.; Bonnesen, P. V. *Anal. Chem.* **2001**, *73*, 1572.
- (4) Xu, D.; Kang, E. T.; Neoh, K. G.; Zhang, Y.; Tay, A. A. O.; Ang, S. S.; Lo, M. C. Y.; Vaidyanathan, K. *J. Phys. Chem. B* **2002**, *106*, 12508.
- (5) Ullman, A. *Chem. Rev.* **1996**, *96*, 1533.
- (6) Linford, M. R.; Fenter, P.; Eisenberger, P. M.; Chidsey, C. E. D. *J. Am. Chem. Soc.* **1995**, *117*, 3145.
- (7) Sieval, A. B.; Demirel, A. L.; Nissink, J. W. M.; Linford, M. R.; van der Maas, J. H.; de Jeu, W. H.; Zuilhof, H.; Sudholter, E. J. R. *Langmuir* **1998**, *14*, 1759.

- (8) Boukherroub, R.; Bensebaa, S. M. F.; Wayner, D. D. M. *Langmuir* **1999**, *15*, 3831.
- (9) Boukherroub, R.; Wayner, D. D. M. *J. Am. Chem. Soc.* **1999**, *121*, 11513.
- (10) Cicero, R. L.; Linford, M. R.; Chidsey, C. E. D. *Langmuir* **2000**, *16*, 5688.
- (11) Buriak, J. M. *Chem. Commun.* **1999**, 1051.
- (12) Zhao, B.; Brittain, W. J. *Prog. Polym. Sci.* **2000**, *25*, 667.
- (13) Kato, K.; Uchida, E.; Kang, E. T.; Uyama, Y.; Ikada, Y. *Prog. Polym. Sci.* **2003**, *28*, 209.
- (14) Jordan, R.; Ulman, A. *J. Am. Chem. Soc.* **1998**, *120*, 243.
- (15) Jordan, R.; Ulman, A.; Kang, J. F.; Rafailovich, M. H.; Sokolov, J. *J. Am. Chem. Soc.* **1999**, *121*, 1016.
- (16) Ingall, M. D. K.; Honeyman, C. H.; Mercure, J. V.; Bianconi, P. A.; Kunz, R. R. *J. Am. Chem. Soc.* **1999**, *121*, 3607.
- (17) Juang, A.; Scherman, O. A.; Grubbs, R. H.; Lewis, N. S. *Langmuir* **2001**, *17*, 1321.
- (18) Kim, N. Y.; Jeon, N. L.; Choi, I. S.; Takami, S.; Harada, Y.; Finnie, K. R.; Girolami, G. S.; Nuzzo, R. G.; Whitesides, G. M.; Laibinis, P. E. *Macromolecules* **2000**, *33*, 2793.
- (19) Weck, M.; Jackiw, J. J.; Rossi, R. R.; Weiss, P. S.; Grubbs, R. H. *J. Am. Chem. Soc.* **1999**, *121*, 4088.
- (20) Prucker, O.; Rühle, J. *Macromolecules* **1998**, *31*, 592.
- (21) Prucker, O.; Rühle, J. *Macromolecules* **1998**, *31*, 602.
- (22) de Boer, B.; Simon, H. K.; Werts, M. P. L.; van der Vegte, E. W.; Hadziioannou, G. *Macromolecules* **2000**, *33*, 349.
- (23) Husseman, M.; Malmström, E. E.; McNamara, M.; Mate, M.; Mecerreyes, D.; Benoit, D. G.; Hedrick, J. L.; Mansky, P.; Huang, E.; Russell, T. P.; Hawker, C. J. *Macromolecules* **1999**, *32*, 1424.
- (24) Ejaz, M.; Yamamoto, S.; Ohno, K.; Tsujii, Y.; Fukuda, T. *Macromolecules* **1998**, *31*, 5934.
- (25) Huang, X.; Wirth, M. J. *Macromolecules* **1999**, *32*, 1694.
- (26) Matyjaszewski, K.; Miller, P. J.; Shukla, N.; Immaraporn, B.; Gelman, A.; Luokala, B. B.; Siclován, T. M.; Kickelbick, G.; Vallant, T.; Hoffmann, H.; Pakula, T. *Macromolecules* **1999**, *32*, 8716.
- (27) Zhao, B.; Brittain, W. J. *J. Am. Chem. Soc.* **1999**, *121*, 3557.
- (28) Yamamoto, S.; Ejaz, M.; Tsujii, Y.; Fukuda, T. *Macromolecules* **2000**, *33*, 5608.
- (29) Zhao, B.; Brittain, W. J.; Zhou, W.; Cheng, S. Z. D. *Macromolecules* **2000**, *33*, 8821.
- (30) Mori, H.; Boker, A.; Krausch, G.; Müller, A. H. E. *Macromolecules* **2001**, *34*, 6871.
- (31) Baum, M.; Brittain, W. J. *Macromolecules* **2002**, *35*, 610.
- (32) Wang, J. S.; Matyjaszewski, K. *Macromolecules* **1995**, *28*, 7901.
- (33) Matyjaszewski, K.; Xia, J. *Chem. Rev.* **2001**, *101*, 2921.
- (34) Zhang, J. F.; Cui, C. Q.; Lim, T. B.; Kang, E. T.; Neoh, K. G. *Chem. Mater.* **1999**, *11*, 1061.
- (35) Zeng F.; Shen Y.; Zhu S.; Pelton R. *Macromolecules* **2000**, *33*, 1628.
- (36) Beamson, G.; Briggs, D. *High-Resolution XPS of Organic Polymers: the Scienta ESCA300 Database*; John Wiley: Chichester, U.K., 1992; p 278.
- (37) Moulder, J. F.; Stickle, W. F.; Sobol, P. E.; Bomben, K. D. In *X-ray Photoelectron Spectroscopy*; Chastian, J., Ed.; Perkin-Elmer: Eden Prairie, MN, 1992; p 43.
- (38) Tan, K. L.; Woon, L. L.; Wong, H. K.; Kang, E. T.; Neoh, K. G. *Macromolecules* **1993**, *26*, 2832.
- (39) Yuk S. H.; Cho S. H.; Lee S. H. *Macromolecules* **1997**, *30*, 6856.
- (40) Zhang, F.; Kang, E. T.; Neoh, K. G.; Huang, W. *J. Biomater. Sci. Polym. Ed.* **2001**, *12*, 515.
- (41) Wang, P.; Tan, K. L.; Kang, E. T.; Neoh, K. G. *J. Mater. Chem.* **2001**, *11*, 2951.
- (42) Pascual, S.; Coutin, B.; Tardi, M.; Polton, K.; Vairon J. P. *Macromolecules* **1999**, *32*, 1432.